*Asian Journal of Chemistry;* *Vol. 38, No. 5 (2026), 1261-1266*

ASIAN JOURNAL OF CHEMISTRY

https://doi.org/10.14233/ajchem.2026.35699

# Synthesis and Biological Evaluation of Indazole Ring Containing Diaryl Urea Derivatives Inducing Activities in Human Breast Cancer MCF-7 Cells

SWETA D. PATEL[1,2,*], HIREN R. CHAUDHARY[3], SHITAL DHIREN FALDU[4], UJASHKUMAR A. SHAH[5], SOHILKHAN DOLATKHAN CHAUHAN[6] and ISHVARCHANDRA PARMAR[7]

[1]Department of Pharmaceutical Chemistry, Nootan Pharmacy College, Sankalchand Patel University, Visnagar-384315, India
[2]Department of Pharmaceutical Chemistry, APMC Pharmacy College, Himatnagar-383001, India
[3]Department of Pharmacology, Manjushree Institute of Pharmacy, Piplaj-382650, India
[4]Department of Pharmaceutical Chemistry, Smt. R.D. Gardi B. Pharmacy College, Rajkot-360110, India
[5]Department of Quality Assurance and Pharmaceutical Chemistry, Nootan Pharmacy College, Sankalchand Patel University, Visnagar-384315, India
[6]Department of Chemistry, Gokul Science College, Gokul Global University, Siddhpur-384151, India
[7]Department of Pharmaceutical Chemistry, SSR College of Pharmacy (Affiliated to Savitribai Phule Pune University, Pune), Silvassa-396230, India

*Corresponding author: E-mail: patelsweta1821989@gmail.com

*Received*: 4 February 2026 *Accepted*: 28 March 2026 *Published online*: 4 May 2026 AJC-22351

In this study, a series of twelve novel indazole-diaryl urea hybrids (**$R_1$-$R_{12}$**) was designed, synthesised and structurally characterised with the aim of developing new breast cancer therapeutics. The synthetic strategy employed a multistep route starting from 5-bromo-1*H*-indazole and afforded the desired derivatives in good yields. The chemical structures of all final products were confirmed using $^1$H and $^{13}$C NMR spectroscopy, FTIR and mass spectrometry, ensuring high purity and structural integrity. *In vitro* cytotoxic activity was assessed against the MCF-7 human breast cancer cell line using the MTT assay. Among the synthesised molecules, compounds **$R_7$**, **$R_8$** and **$R_{11}$** emerged as the most active, with $IC_{50}$ values of 13.15, 12.71 and 11.48 μM, respectively. Notably, these values represent a significant improvement compared to the reference drug sorafenib ($IC_{50}$ = 29.3 μM). Structure–activity relationship (SAR) analysis suggested that electron-withdrawing substituents such as fluorine and chlorine, as well as di-substituted aromatic rings, enhanced cytotoxic potency. Molecular docking studies were performed on the histone deacetylase crystal structure (HDAC, PDB ID: 4LXZ) to provide structural insights into binding affinity. The most potent compounds displayed favourable docking scores (**$R_7$** = -10.1 kcal/mol and **$R_{11}$** = -9.5 kcal/mol) and established key hydrogen bonding and hydrophobic interactions with active site residues, validating the experimental data. In addition, *in silico* ADME profiling using SwissADME demonstrated compliance with Lipinski's rule of five, favourable log P values and suitable topological polar surface area (TPSA), indicating good oral bioavailability and drug-likeness. Taken together, these results demonstrate that indazole-diaryl urea hybrids, particularly compounds **$R_7$**, **$R_8$** and **$R_{11}$**, possess significant cytotoxic potential against breast cancer cells and outperform sorafenib *in vitro*. The combined experimental and computational data highlight these compounds as promising lead scaffolds for further optimisation and development of next-generation anticancer therapeutics.

**Keywords: Indazole, Diaryl urea, MCF-7, Cytotoxicity, Histone deacetylase, Molecular docking, ADME.**

## INTRODUCTION

Heterocyclic scaffolds are important in medicinal chemistry due to their structural diversity and ability to form non-covalent interactions such as hydrogen bonding, π-π stacking and hydrophobic contacts, enabling efficient target binding [1,2]. Substituted heterocycles further enhance pharmacokinetic properties and binding affinity, with indazole derivatives receiving particular attention.

The indazole framework, a fused pyrazole-benzene bicyclic system, offers planar geometry and tunable electronic properties that support diverse chemical modifications [3,4]. Indazole derivatives exhibit various biological activities including anti-inflammatory, antimicrobial and anticancer effects, with reported cytotoxicity against breast, lung and colon cancer cell lines [5,6]. Substituent variations such as electron-withdrawing or electron-donating groups further modulate biological activity by influencing lipophilicity, electronic distribution and hydrogen-bonding interactions [7].

In parallel, the diaryl urea moiety represents another pharmacophore of great therapeutic interest. Diaryl urea derivatives are well-known for their ability to inhibit kinase pathways, angiogenesis and cell proliferation [8,9]. The urea linker enables hydrogen bonding with enzyme residues, while aromatic substituents enhance hydrophobic and π-π stacking interactions, contributing to improved binding affinities and biological activities [10].

Breast cancer remains one of the most prevalent malignancies and a leading cause of mortality among women worldwide. Limitations of current therapies including resistance and toxicity, highlight the need for novel chemo-therapeutic agents targeting key cancer-related pathways [11,12]. The combination of indazole and diaryl urea moieties into hybrid molecules is therefore a promising strategy to generate compounds with synergistic pharmacological properties. By merging two biologically validated pharmacophores, the resulting hybrids are expected to achieve enhanced cytotoxic effects through multiple binding interactions at the active site of cancer-related targets. To test this hypothesis, we designed and synthesised a focused library of twelve indazole-diaryl urea hybrids (**$R_1$-$R_{12}$**) using a multistep synthetic approach.

The synthesised compounds were subjected to the structural characterisation using spectroscopic and spectrometric techniques including $^1$H and $^{13}$C NMR and mass spectrometry. Their cytotoxic activity was evaluated against the MCF-7 human breast cancer cell line using the MTT assay and results were benchmarked against sorafenib. To rationalize the biological findings, molecular docking was carried out using the histone deacetylase (HDAC) crystal structure (PDB ID: 4LXZ), which provided insights into binding modes, interaction profiles and docking scores. Furthermore, drug-likeness and physicochemical properties were assessed through *in silico* ADME profiling.

## EXPERIMENTAL

All reagents and solvents were of analytical grade and procured from Avra Synthesis Pvt. Ltd., Finar Chemicals and Spectrochem Pvt. Ltd., India. All reactions were monitored by thin-layer chromatography (TLC) using silica gel 60 $F_{254}$ pre-coated plates (0.2 mm, Merck). Visualisation was done under UV light or by exposure to iodine vapours. Column chromatography was performed using silica gel (60-120 mesh) with appropriate solvent systems. Melting points were determined by the open capillary method and are uncorrected. FTIR spectra were recorded using a Shimadzu FTIR-8400 spectrophotometer in ATR mode. $^1$H and $^{13}$C NMR spectra were acquired on a Bruker Avance II spectrometer operating at 400 MHz and 101 MHz, respectively, using DMSO-$d_6$ as solvent and tetramethylsilane (TMS) as the internal reference. Mass spectra were recorded on a JEOL-JMSD-300 spectrometer at 70 eV.

**Synthesis of indazole-diaryl urea derivatives ($R_1$-$R_{12}$):** A new series of indazole-diaryl urea derivatives (**$R_1$-$R_{12}$**) was successfully synthesised through a multisteps reaction route, beginning from 5-bromo-1*H*-indazole as the key starting material. Initially, 5-bromo-1*H*-indazole was protected with 2-(trimethylsilyl)-ethoxymethyl chloride (SEM-chloride) using NaH in DMF at 0 ºC under $N_2$ atmosphere, followed by the extraction and purification to obtain the protected intermediate. Palladium-catalysed coupling with an aryl halide using XPhos and $Pd_2(dba)_3$ in 1,4-dioxane afforded the arylated indazole derivative, which was subsequently deprotected with 4 M HCl in dioxane to obtain the free amine. The amine was reacted with substituted anilines in THF using triphosgene and triethylamine to form diaryl urea intermediates [13,14]. Final deprotection with triflic acid in dichloromethane provided the indazole-diaryl urea derivatives (**$R_1$-$R_{12}$**) (**Scheme-I**), which were purified by column chromatography.

**1-(1-(1*H*-Indazol-5-yl)piperidin-4-yl)-1-methyl-3-(1-methyl-2-oxo-5-(trifluoromethyl)-1,2-dihydropyridin-3-yl)urea ($R_1$):** Yield: 43.02%; $^1$H NMR (400 MHz, DMSO, δ ppm): 3.34 (s, 3H, $CH_3$), 3.37 (s, 3H, $CH_3$), 6.0 (s, 1H, CONH), 6.38 (s, 1H, ArH), 6.67 (d, 1H, ArH), 8.14-8.20 (t, 1H, ArH), 7.89 (s, 1H, ArH), 1.60, 1.85 (m, 2H, $CH_2$), 2.91, 3.01 (m, 2H, $CH_2$), 12.4 (d, 1H, ArNH indazole ring); $^{13}$C NMR (101 MHz, DMSO, δ ppm): 26.8 (X2), 29.7, 39.7, 51.4 (X2), 65.3, 99.1, 114.5, 116.0, 117.6, 120.5, 124.9, 127.4, 129.7 (X2), 131.8, 134.2, 136.1, 150.4 (C=O), 158.6 (C=O); ESI-MS *m/z*: 449.34 [M $^+$1].

**1-(1-(1*H*-Indazol-5-yl)piperidin-4-yl)-1-methyl-3-phenylurea ($R_2$):** Yield: 51.48%: $^1$H NMR (400 MHz, DMSO, δ ppm): 12.4 (s, 1H, ArNH indazole ring), 8.14-8.20 (m, 1H, ArH), 7.43-7.61 (m, 1H, ArH), 7.19-7.61 (m, 1H, ArH), 1.85 (d, 2H, $CH_2$), 3.47 (s, 3H, $CH_3$); $^{13}$C NMR (101 MHz, DMSO, δ ppm): 26.8 (X2), 51.4 (X2), 65.2, 99.1, 114.5, 117.6, 121.6 (X2), 124.9, 128.0, 128.9 (X2), 129.4, 134.2, 136.1, 139.4, 155.1 (C=O); ESI-MS *m/z*: 350.19 $[M+H]^+$.

**1-(1-(1*H*-Indazol-5-yl)piperidin-4-yl)-3-(4-hydroxyphenyl)-1-methylurea ($R_3$):** Yield: 53.18%, $^1$H NMR (400 MHz, DMSO, δ ppm): 12.4 (s, 1H, ArNH indazole ring), 8.14-8.20 (d, 1H, ArH), 7.45 (d, 1H, ArH), 7.18 (s, 1H, ArH), 6.93 (d, 1H, ArH), 6.67 (s, 1H, ArH), 6.0 (s, 1H, CONH), 5.35 (s, 1H, ArOH), 3.60 (m, 3H, ArH), 3.47 (s, 3H, $CH_3$), 2.91-3.01 (m, 1H, $CH_2$), 1.60, 1.85 (m, 1H, $CH_2$); $^{13}$C NMR (101 MHz, DMSO, δ ppm): 29.3 (X2), 50.0, 51.4 (X2), 99.1, 114.5, 116.1, 117.6, 123.0 (X2), 124.9, 129.4, 132.0, 134.2, 136.1, 154.1, 154.3 (C=O); ESI-MS *m/z*: 366.19 $[M+H]^+$.

**1-(1-(1*H*-Indazol-5-yl)piperidin-4-yl)-3-(4-fluorophenyl)-1-methylurea ($R_4$):** Yield: 48.54%; $^1$H NMR (400 MHz, DMSO, δ ppm): 12.4 (s, 1H, ArNH indazole ring), 6.0 (s, 2H, CONH), 8.14-8.20 (d, 1H, ArH), 7.60 (d, 1H, ArH), 7.22 (d, 1H, ArH), 6.67 (t, 1H, ArH), 1.85 (m, 2H, $CH_2$), 1.59 (m, 2H, $CH_2$), 2.91-3.01 (m, 1H, $CH_2$); $^{13}$C NMR (101 MHz, DMSO, δ ppm): 26.8 (X2), 29.2, 51.4 (X2), 65.2, 99.1, 114.5, 115.7, 117.6, 119.3 (X2), 124.9, 129.4, 134.2, 135.0, 136.1, 155.1 (C=O), 162.9; ESI-MS *m/z*: 350.19 $[M+H]^+$.

**1-(1-(1*H*-Indazol-5-yl)piperidin-4-yl)-3-(3,5-dichlorophenyl)-1-methylurea ($R_5$):** Yield: 38.25%; $^1$H NMR (400 MHz, DMSO, δ ppm): 12.4 (s, 1H, ArNH indazole ring), 6.0 (s, 2H, CONH), 3.47 (s, 3H, $CH_3$), 1.85, 1.60 (m, 2H, $CH_2$), 2.91-3.01 (m, 2H, $CH_2$), 3.60 (t, 1H, ArH), 6.67 (d, 1H, ArH), 7.18 (s, 1H, ArH), 7.43 (s, 1H, ArH), 7.83 (d, 1H, ArH), 8.14-8.20 (d, 1H, ArH); $^{13}$C NMR (101 MHz, DMSO, δ ppm): 26.8 (X2), 29.2, 51.4 (X2), 65.2, 99.1, 114.5, 117.6, 120.1 (X2), 124.9 (X2), 129.2 (X2), 134.2, 136.1, 138.7, 155.1 (C=O), ESI-MS *m/z*: 419.2 [M $^+$1].

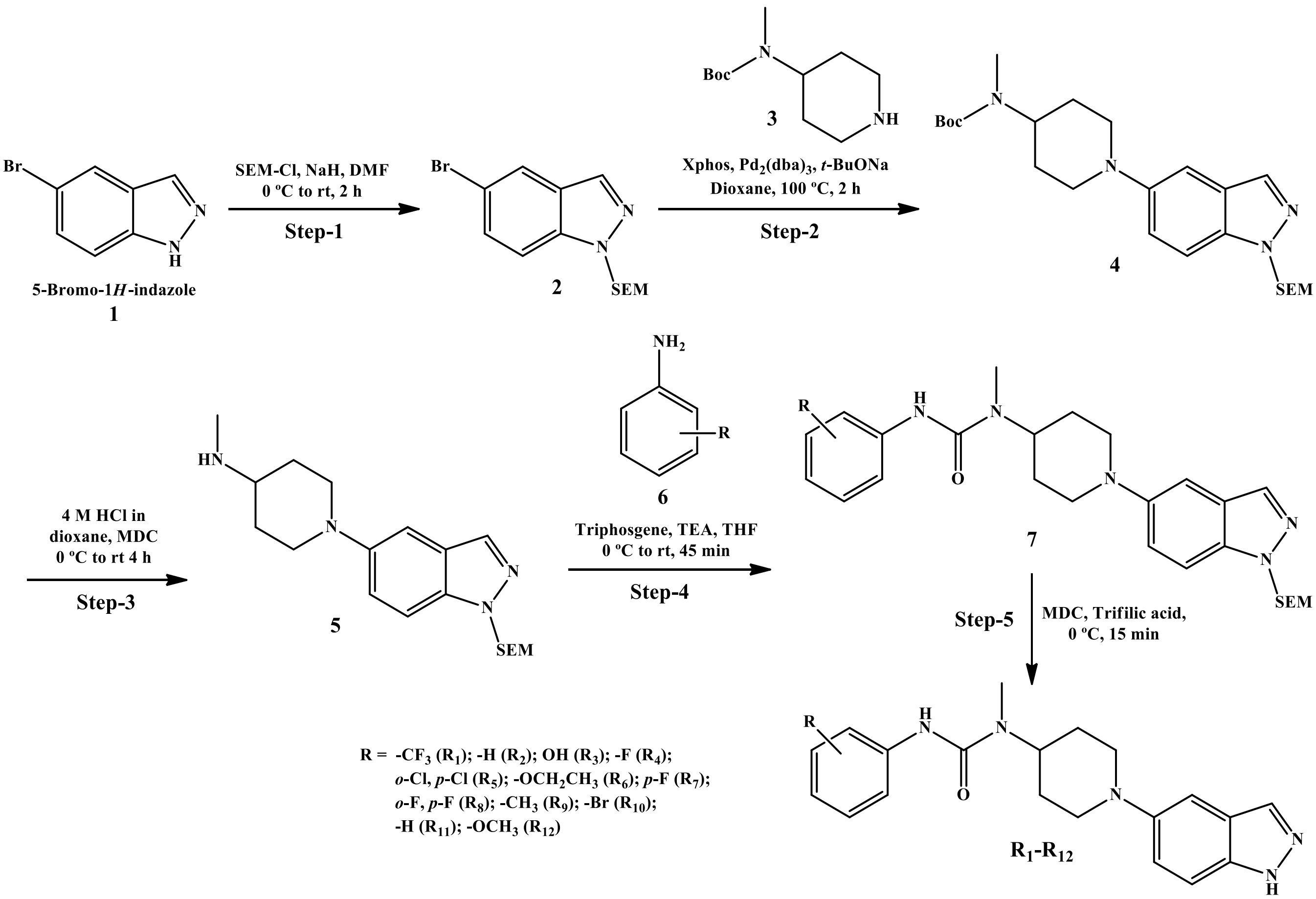

**Scheme-I:** Synthesis of diaryl urea fused indazole derivatives

**1-(1-(1*H*-Indazol-5-yl)piperidin-4-yl)-3-(2-ethoxyphenyl)-1-methylurea (R6):** Yield: 54.35%; $^1$H NMR (400 MHz, DMSO, δ ppm): 12.4 (s, 1H, ArNH indazole ring), 6.0 (s, 2H, CONH), 3.47 (s, 3H, $CH_3$), 8.20 (d, 1H, ArH), 2.91-3.01 (m, 1H, $CH_2$), 1.85 (m, 2H, $CH_2$), 1.59 (m, 2H, $CH_2$), 7.18 (d, H, ArH), 7.08 (m, 1H, ArH), 7.85 (d, 1H, ArH), 6.99 (d, 1H, ArH), 1.32 (s, 3H, $CH_3$), 4.09 (m, 1H, $CH_2$); $^{13}$C NMR (101 MHz, DMSO, δ ppm): 14.8. 26.8 (X2), 29.2, 51.4 (X2), 64.6, 65.2, 99.1, 112.9, 114.5, 117.6, 119.9, 120.5, 124.3, 124.9, 127.8, 129.4, 134.2, 136.1, 155.1 (C=O), 155.6 (C=O); ESI-MS *m/z*: 394.22 [M+H]$^+$.

**1-(1-(1*H*-Indazol-5-yl)piperidin-4-yl)-3-(3-fluorophenyl)-1-methylurea (R7):** Yield: 50.79%; $^1$H NMR (400 MHz, DMSO, δ ppm): 12.4 (s, 1H, ArNH indazole ring), 6.0 (s, 2H, CONH), 3.47 (s, 3H, $CH_3$), 8.20 (m, 1H, ArH), 2.91-3.01 (m, 1H, $CH_2$), 1.85 (m, 2H, $CH_2$), 1.59 (m, 2H, $CH_2$), 7.18 (d, H, ArH), 3.60 (m, 1H, ArH), 7.75 (d, 1H, ArH), 6.67 (s, 1H, ArH), 1.32 (s, 3H, $CH_3$), 4.09 (m, 1H, $CH_2$), 8.14 (m, 1H, ArH), 7.38-7.41 (m, 1H, ArH), 6.98 (m, 1H, ArH); $^{13}$C NMR (400 MHz, DMSO, δ ppm): 26.8 (X2), 29.2, 51.4 (X2), 65.2, 99.1, 114.5, 116.5, 117.6, 124.9, 129.4, 130.5, 134.2, 136.1, 137.5, 155.1 (C=O), 163.1; ESI-MS *m/z*: 368.18 [M+H]$^+$.

**1-(1-(1*H*-Indazol-5-yl)piperidin-4-yl)-3-(3,5-difluorophenyl)-1-methylurea (R8):** Yield: 50.17%; $^1$H NMR (400 MHz, DMSO, δ ppm): 12.4 (s, 1H, ArNH indazole ring), 6.0 (s, 2H, CONH), 3.47 (s, 3H, $CH_3$), 8.20 (t, 1H, ArH), 2.91-3.01 (m, 1H, $CH_2$), 1.85 (m, 2H, $CH_2$), 1.59 (m, 2H, $CH_2$), 7.18 (s, H, ArH), 3.60 (m, 1H, ArH), 7.52 (d, 1H, ArH), 6.42 (m, 1H, ArH), 8.14 (t, 1H, ArH), 7.38-7.41 (m, 1H, ArH), 6.98 (m, 1H, ArH); $^{13}$C NMR (101 MHz, DMSO, δ ppm): 26.8 (X2), 29.2, 51.4 (X2), 65.2, 99.1, 100.3, 112.1 (X2), 114.5, 117.6, 124.9, 129.4, 134.2, 136.1, 139.1, 155.1 (C=O), 157.9 (X2); ESI-MS *m/z*: 368.17 [M+H]$^+$.

**1-(1-(1*H*-Indazol-5-yl)piperidin-4-yl)-1-methyl-3-(*m*-tolyl)urea (R9):** Yield: 66.79%; $^1$H NMR (400 MHz, DMSO, δ ppm): 12.4 (s, 1H, ArNH indazole ring), 6.0 (s, 2H, CONH), 3.47 (s, 3H, $CH_3$), 8.20 (m, 1H, ArH), 2.91-3.01 (m, 1H, $CH_2$), 1.85 (m, 2H, $CH_2$), 1.59 (m, 2H, $CH_2$), 7.18 (d, H, ArH), 3.60 (m, 1H, ArH), 7.75 (d, 1H, ArH), 6.67 (s, 1H, ArH), 1.32 (s, 3H, $CH_3$), 4.09 (m, 1H, $CH_2$), 8.14 (m, 1H, ArH), 7.38-7.41 (m, 1H, ArH), 6.98 (m, 1H, ArH); $^{13}$C NMR (DMSO) δ ppm: 21.3, 26.8 (X2), 29.2, 51.4 (X2), 65.2, 99.1, 114.5, 117.6, 118.6, 124.6, 124.9, 128.8, 129.4, 134.2, 135.8, 136.1, 138.6, 155.1 (C=O); ESI-MS *m/z*: 364.21 [M+H]$^+$.

**1-(1-(1*H*-Indazol-5-yl)piperidin-4-yl)-3-(3-bromophenyl)-1-methylurea (R10):** Yield: 32.60%; $^1$H NMR (400 MHz, DMSO, δ ppm): 12.4 (s, 1H, ArNH indazole ring), 6.0 (s, 2H, CONH), 3.47 (s, 3H, $CH_3$), 8.20 (s, 1H, ArH), 2.91-3.01 (m, 1H, $CH_2$), 1.60-1.85 (m, 2H, $CH_2$), 7.18 (d, H, ArH), 3.60 (m, 1H, ArH), 7.75 (d, 1H, ArH), 6.67 (s, 1H, ArH), 7.87 (s, 1H, ArH), 8.14 (s, 1H, ArH), 7.34 (s, 1H, ArH); $^{13}$C NMR (400 MHz, DMSO, δ ppm): 26.8 (X2), 29.2, 51.4, 65.2, 99.1, 114.5, 117.6, 120.8, 123.3, 124.9, 127.2, 129.4, 130.0, 134.2, 136.1, 138.1, 155.1 (C=O); ESI-MS *m/z*: 428.10 $[M+H]^+$.

**1-((1-(1*H*-Indazol-5-yl)piperidin-4-yl)(methyl)carbamoyl)benzamide ($R_{11}$):** Yield: 37.50%; $^1$H NMR (400 MHz, DMSO, δ ppm): 12.4 (s, 1H, ArNH indazole ring), 10.0 (s, 2H, CONH), 3.47 (s, 3H, $CH_3$), 8.20 (s, 1H, ArH), 2.91-3.01 (m, 1H, $CH_2$), 1.60-1.85 (m, 2H, $CH_2$), 7.18 (s, H, ArH), 3.60 (m, 1H, ArH), 7.63-7.70 (m, 1H, ArH), 6.67 (d, 1H, ArH), 7.87 (s, 1H, ArH), 8.14 (s, 1H, ArH), 8.03 (s, 1H, ArH); $^{13}$C NMR (101 MHz, DMSO, δ ppm): 26.8 (X2), 28.9, 51.4, 64.9, 99.1, 114.5, 117.6, 124.9, 127.5 (X2), 128.8 (X2), 129.4, 132.1, 133.2, 134.2, 136.1, 153.8 (C=O), 167.2 (C=O), ESI-MS *m/z*: 378.3 $[M^+1]$.

**1-(1-(1*H*-Indazol-5-yl)piperidin-4-yl)-3-(4-methoxyphenyl)-1-methylurea ($R_{12}$):** Yield: 44.78%; $^1$H NMR (400 MHz, DMSO, δ ppm): 12.4 (s, 1H, ArNH indazole ring), 6.0 (s, 2H, CONH), 3.47 (s, 3H, $CH_3$), 8.20 (t, 1H, ArH), 2.91-3.01 (m, 1H, $CH_2$), 1.60-1.85 (m, 2H, $CH_2$), 7.18 (s, H, ArH), 3.60 (m, 1H, ArH), 7.51 (d, 1H, ArH), 6.97 (d, 1H, ArH), 6.67 (d, 1H, ArH), 7.51 (d, 1H, ArH), 8.14 (s, 1H, ArH), 7.34 (s, 1H, ArH), 3.87 (s, 3H, $CH_3$); $^{13}$C NMR (101 MHz, DMSO, δ ppm): 26.8 (X2), 29.2, 51.4 (X2), 55.8, 65.2, 99.1, 114.5 (X3), 117.6, 119.8 (X2), 124.9, 129.4, 131.7, 134.2, 136.1, 155.1 (C=O), 158.9; ESI-MS *m/z*: 380.20 $[M+H]^+$.

**Cell culture and *in vitro* cytotoxicity evaluation**: The anticancer activity of the synthesised compounds (**$R_1$-$R_{12}$**) was evaluated in MCF-7 human breast adenocarcinoma cells obtained from NCCS, Pune, India. Cells were cultured in MEM supplemented with 10% FBS and antibiotics at 37 ºC in 5% $CO_2$. Stock solutions of the compounds were prepared in DMSO and diluted with culture medium, maintaining final DMSO concentration below 0.1%. Cytotoxicity was assessed using the MTT assay by seeding MCF-7 cells ($2 \times 10^4$ cells/well) in 96-well plates, followed by treatment with compounds (1-100 μM) for 24 h. After incubation with MTT solution, the formed formazan crystals were dissolved in DMSO and absorbance was measured at 570 nm using a microplate reader [15,16]. The percentage of viable cells was calculated relative to untreated control cells using the eqn. 1:

$$\text{Cell viability (\%)} = \frac{\text{Abs}_{\text{sample}}}{\text{Abs}_{\text{control}}} \times 100 \quad (1)$$

The half-maximal inhibitory concentration ($IC_{50}$) values were obtained from dose–response curves plotted using GraphPad Prism 8 software. Sorafenib was used as the reference standard for comparison. All experiments were carried out in triplicate and the results were expressed as mean ± standard deviation (SD).

**Molecular docking and ADME analysis:** Molecular docking studies were performed to investigate the interaction profile and binding affinity of the synthesised indazole-diaryl urea derivatives with the crystal structure of histone deacetylase (HDAC, PDB ID: 4LXZ). The protein was prepared by removing water molecules and adding hydrogen atoms using Schrödinger's protein preparation wizard. Ligand structures were drawn in ChemDraw and energy-minimised using the OPLS4 force field in Maestro. Docking was performed using the Glide module in extra-precision (XP) mode and the top-ranked poses were analysed based on docking score, hydrogen bond interactions and hydrophobic contacts within the active site pocket. Visualisation and interpretation of interactions were carried out using Maestro and PyMOL software.

*In silico* prediction of physico-chemical and pharmacokinetic parameters was carried out using the SwissADME online platform to evaluate the drug-likeness and bioavailability of the synthesised compounds. Parameters such as molecular weight, hydrogen bond donors and acceptors, partition coefficient (log P), aqueous solubility (log S), topological polar surface area (TPSA) and number of rotatable bonds were calculated. Lipinski's rule of five and Veber's rule were used as reference criteria to assess oral bioavailability and drug-likeness.

**Statistical analysis:** All biological data were expressed as mean ± standard deviation (SD) from at least three independent experiments. Statistical analysis was performed using one-way ANOVA followed by Tukey's post hoc test, with $p < 0.05$ considered statistically significant. Dose-response curves and $IC_{50}$ values were calculated using GraphPad Prism 8 software.

## RESULTS AND DISCUSSION

A new library of twelve indazole-urea derivatives (**$R_1$-$R_{12}$**) was successfully synthesised and characterised to confirm their chemical structures and purity. The synthetic design was focused on incorporating the indazole nucleus, a privileged heterocycle known for anticancer properties, with a urea pharmacophore capable of establishing multiple hydrogen-bonding interactions with biological targets such as histone deacetylase (HDAC). The purity and reproducibility of all synthesised molecules were confirmed by sharp melting points and single-spot TLC profiles.

All compounds were obtained in moderate to good yields (32-67%) and were characterised comprehensively by FTIR, $^1$H NMR, $^{13}$C NMR and ESI-MS spectroscopy. The analytical data were in excellent agreement with the proposed structures, confirming the successful formation of the desired urea-linked indazole scaffolds. In the $^1$H NMR spectra, each compound exhibited a distinctive singlet at δ ~6.0 ppm corresponding to the urea NH proton, while the indazole NH proton consistently appeared as a singlet near δ 12.4 ppm, confirming the retention of the indazole framework. The aromatic region (δ 6.5-8.3 ppm) showed multiple signals consistent with the substitution pattern of the phenyl moiety attached to the urea linker. Methyl substituents appeared as singlets around δ 3.3-3.5 ppm, while methoxy or ethoxy groups were represented by peaks at δ 3.8-4.1 ppm. The characteristic methylene protons of the piperidine ring were observed as multiplets between δ 1.5-3.0 ppm, indicating the successful incorporation of the cyclic amine spacer.

The $^{13}$C NMR spectra of the synthesised derivatives (**$R_1$-$R_{12}$**) exhibited characteristic carbonyl signals corresponding to the urea functionality. The urea carbonyl carbon appeared in the range of δ 153-158 ppm, consistent with the expected chemical shift for diaryl urea derivatives, while compounds containing additional amide functionalities showed signals in the δ 165-168 ppm region. Aromatic carbons were observed between δ 110-140 ppm, corresponding to the indazole and substituted phenyl rings. Substituents such as fluorine, chlorine and trifluoromethyl groups induced slight downfield shifts due to their electron-withdrawing effects. The ESI-MS spectra further confirmed the molecular integrity of the synthesised compounds. Each derivative exhibited a clear $[M+H]^+$ molecular ion peak consistent with its calculated molecular weight. For example, compound $\mathbf{R_1}$ showed *m/z* 449.34 $[M+H]^+$, $\mathbf{R_4}$ showed *m/z* 350.19 $[M+H]^+$, $\mathbf{R_8}$ showed *m/z* 368.17 $[M+H]^+$ and $\mathbf{R_{11}}$ showed *m/z* 378.30 $[M+H]^+$, which are in good agreement with their expected molecular masses.

Among the series, $\mathbf{R_1}$, containing a trifluoromethyl group, displayed distinct spectral features due to the strong electron-withdrawing effect of $CF_3$, causing a noticeable downfield shift of aromatic and carbonyl signals. Fluorinated analogues ($\mathbf{R_4}$, $\mathbf{R_7}$, $\mathbf{R_8}$) exhibited characteristic C-F coupling effects in both proton and carbon spectra, while $\mathbf{R_3}$ (4-hydroxyphenyl) showed a diagnostic phenolic OH singlet at δ 5.35 ppm. Compounds bearing halogen substituents such as chlorine or bromine ($\mathbf{R_5}$ and $\mathbf{R_{10}}$) displayed molecular ion peaks at *m/z* 419.2 and 428.10, respectively, consistent with isotopic patterns typical of halogen-containing molecules.

***In vitro* anticancer activity:** The cytotoxic activity of the synthesised indazole-diaryl urea derivatives ($\mathbf{R_1}$-$\mathbf{R_{12}}$) was evaluated against the human breast adenocarcinoma cell line (MCF-7) using the standard MTT assay. Sorafenib, a well-established diaryl urea-based multikinase inhibitor, was used as a reference standard for comparison. The $IC_{50}$ values were calculated from the dose-response curves obtained after 24 h exposure and the results are summarised in Table-1.

TABLE-1
*In vitro* ANTI-CANCER ACTIVITY DATA OF SYNTHESISED INDAZOLE-DIARYL UREA DERIVATIVES ($\mathbf{R_1}$-$\mathbf{R_{12}}$)

| Compd. | $IC_{50}$ (μM) | Compd. | $IC_{50}$ (μM) |
|---|---|---|---|
| $\mathbf{R_1}$ | 18.39 | $\mathbf{R_7}$ | 13.15 |
| $\mathbf{R_2}$ | 21.13 | $\mathbf{R_8}$ | 12.71 |
| $\mathbf{R_3}$ | 22.37 | $\mathbf{R_9}$ | 17.12 |
| $\mathbf{R_4}$ | 12.39 | $\mathbf{R_{10}}$ | 25.12 |
| $\mathbf{R_5}$ | 14.07 | $\mathbf{R_{11}}$ | 11.48 |
| $\mathbf{R_6}$ | 12.10 | $\mathbf{R_{12}}$ | 15.36 |
| | | Sorafenib | 29.3 |

All the synthesised compounds exhibited measurable cytotoxic effects with $IC_{50}$ values ranging between 11.48 and 25.12 μM. The results were obtained from three independent experiments and are expressed as mean ± standard deviation (S.D.). Statistical analysis was performed using one-way ANOVA followed by Tukey's post-hoc test, with $p < 0.05$ considered statistically significant.

Among the series, $\mathbf{R_7}$ (*p*-F), $\mathbf{R_8}$ (*o*-F, *p*-F) and $\mathbf{R_{11}}$ (–H) displayed the most potent inhibition of MCF-7 cell proliferation, with $IC_{50}$ values of 13.15, 12.71 and 11.48 μM, respectively. These compounds were found to be significantly more active than standard sorafenib ($IC_{50}$ = 29.3 μM), indicating enhanced potency conferred by the hybrid indazole-diaryl urea scaffold. Moderate activity was observed for $\mathbf{R_5}$ (*o*-Cl, *p*-Cl) ($IC_{50}$ = 14.07 μM) and $\mathbf{R_4}$ (–F) ($IC_{50}$ = 12.39 μM), while electron-donating groups such as -$OCH_3$ ($\mathbf{R_{12}}$, $IC_{50}$ = 15.36 μM) and -$CH_3$ ($\mathbf{R_9}$, $IC_{50}$ = 17.12 μM) slightly decreased cytotoxic potency. The least active compounds were $\mathbf{R_3}$ (-OH) and $\mathbf{R_{10}}$ (-Br), with $IC_{50}$ values above 20 μM. The observed trend highlights the importance of electronic effects in modulating anticancer activity.

**Structure-activity relationship (SAR):** SAR analysis indicated that both electronic and steric effects of aromatic substituents strongly influenced cytotoxic potency. Compounds bearing electron-withdrawing groups, particularly fluorine and chlorine, showed higher activity than electron-donating analogues. Fluorinated derivatives ($\mathbf{R_7}$ and $\mathbf{R_8}$) improved lipophilicity, metabolic stability and ligand-protein interactions, while the difluoro substitution in $\mathbf{R_8}$ (*o*-F, *p*-F) provided an optimal balance of hydrophobic and electronic effects, resulting in enhanced cell growth inhibition.

Steric bulk influences target binding as dichloro-substituted $\mathbf{R_5}$ demonstrated good potency ($IC_{50}$ = 14.07 μM) but was slightly less active than fluoro analogues, possibly due to steric hindrance around the urea linkage restricting optimal orientation within the HDAC binding pocket. Electron-donating groups reduce potency which is shown by the presence of -OH or -$OCH_3$ groups ($\mathbf{R_3}$ and $\mathbf{R_{12}}$) led to lower activity, likely due to increased electron density on the aromatic ring, which reduces the electrophilicity of the urea carbonyl group and weakens hydrogen bonding with target residues. Moreover, polar substituents may engage in solvent hydrogen bonding, thereby diminishing binding affinity at the hydrophobic pocket of HDAC. Unsubstituted analogue retains strong baseline activity as the unsubstituted compound $\mathbf{R_{11}}$ exhibited strong activity ($IC_{50}$ = 11.48 μM), suggesting that the indazole-diaryl urea core itself possesses intrinsic cytotoxic potential, possibly through dual engagement with kinase and HDAC targets, as seen in similar scaffolds reported in literature [17]. These findings establish that the electron-withdrawing substituents, especially fluorine, play a key role in strengthening the biological activity of these compounds.

***In silico* ADME and drug-likeness evaluation:** To predict the pharmacokinetic and physico-chemical properties of the synthesised compounds, ADME analyses were performed using the SwissADME web tool. All compounds exhibited drug-like characteristics with no violations of Lipinski's rule of five, depicted in Table-2.

The calculated molecular weights were below 500 Da, and hydrogen bond donors and acceptors ranged from 2-3 and 4-6, respectively, remaining within acceptable limits for oral drug candidates. Predicted log P values (1.87-4.67) indicate balanced lipophilicity, supporting membrane permeability and bioavailability, while aqueous solubility (log S) values between -4.07 and -5.44 correspond to moderately soluble lipophilic compounds. TPSA values below 90 $Å^2$ suggest efficient passive diffusion across cell membranes. The limited number of rotatable bonds (≤ 8) and moderate molecular flexibility are consistent with favourable oral absorption. None of the compounds were predicted to cross the blood-brain barrier, which is advantageous for anticancer agents targeting peripheral tissues. These ADME parameters indicate suitable physico-chemical properties, structural stability and predicted absorption characteristics, supporting further *in vivo* pharmacological evaluation.

## Conclusion

A library of indazole-diaryl urea derivatives ($\mathbf{R_1}$-$\mathbf{R_{12}}$) was successfully designed, synthesised and structurally characterised, confirming the formation of the intended scaffolds with

TABLE-2
ADME PREDICTION OF SYNTHESISED INDAZOLE-DIARYL UREA DERIVATIVES (**$R_1$-$R_{12}$**)

| Compound | Log P | TPSA (Å$^2$) | Log S | HBD | HBA | BBB | CYP1A2 inhibition | GIA | Lipinski filter |
|---|---|---|---|---|---|---|---|---|---|
| **$R_1$** | 2.05 | 74.29 | -4.13 | 3 | 2 | -1.485 | No | Low | Yes; 0 violation |
| **$R_2$** | 2.62 | 64.26 | -4.19 | 2 | 2 | -1.486 | No | High | Yes; 0 violation |
| **$R_3$** | 1.87 | 84.49 | -4.23 | 3 | 3 | -1.428 | No | High | Yes; 0 violation |
| **$R_4$** | 2.77 | 64.26 | -5.44 | 2 | 3 | -1.397 | No | High | Yes; 0 violations |
| **$R_5$** | 4.67 | 64.26 | -4.67 | 2 | 2 | -1.559 | No | High | Yes; 0 violations |
| **$R_6$** | 3.04 | 73.49 | -4.23 | 2 | 3 | -1.632 | No | High | Yes; 0 violation |
| **$R_7$** | 3.01 | 64.26 | -4.34 | 2 | 3 | -1.719 | No | High | Yes; 0 violation |
| **$R_8$** | 3.44 | 64.26 | -4.13 | 2 | 4 | -1.667 | No | High | Yes; 0 violations |
| **$R_9$** | 2.68 | 64.26 | -4.98 | 2 | 2 | -1.859 | No | High | Yes; 0 violations |
| **$R_{10}$** | 3.25 | 64.26 | -4.98 | 2 | 2 | -1.719 | Yes | High | Yes; 0 violations |
| **$R_{11}$** | 2.32 | 81.33 | -4.07 | 2 | 3 | -1.667 | No | High | Yes; 0 violations |
| **$R_{12}$** | 2.63 | 73.49 | -4.14 | 2 | 3 | -1.859 | No | High | Yes; 0 violations |

TPSA: total polar surface area, GIA: Gastrointestinal absorbance, HBD: Hydrogen bond donor, HBA: Hydrogen bond acceptor, BBB: Blood Brain Barrier

good purity and reproducibility. Spectroscopic analyses ($^1$H/$^{13}$C NMR and ESI-MS) verified the presence of key functional features, including the indazole core and urea linkage, supporting the structural integrity of the synthesised compounds. The cytotoxic evaluation against MCF-7 breast cancer cells demonstrated that several derivatives exhibited significant antiproliferative activity, with compounds **$R_7$**, **$R_8$** and **$R_{11}$** showing enhanced potency compared to the reference drug. Structure–activity relationship analysis indicated that electron-withdrawing substituents particularly fluorine, improved biological activity, while steric and electronic factors influenced binding interactions and cytotoxic response. *In silico* ADME predictions revealed favourable drug-like properties, including acceptable molecular weight, balanced lipophilicity, suitable polarity and predicted oral absorption, supporting the pharmacokinetic suitability of the series. These findings highlight the indazole-diaryl urea scaffold as a promising framework for anticancer drug development and provide a basis for investigations and *in vivo* evaluation.

## ACKNOWLEDGEMENTS

This research was supported by Sankalchand Patel University, Visnagar, India, for this research work.

## CONFLICT OF INTEREST

The authors declare that there is no conflict of interests regarding the publication of this article.

## DECLARATION OF AI-ASSISTED TECHNOLOGIES

During the preparation of this manuscript, the authors used an AI-assisted tool(s) to improve the language. The authors reviewed and edited the content and take full responsibility for the published work.

## REFERENCES

1. S.A. Ahmed, A.S. Chopde, A.B. Yamnaji and N.S. Pinjari, *J. Pharma Insights Res.*, **3**, 394 (2025); https://doi.org/10.69613/yj37ha36
2. I. Pibiri, *Int. J. Mol. Sci.*, **25**, 9503 (2024); https://doi.org/10.3390/ijms25179503
3. T. Gallavardin and X. Franck, *Org. Biomol. Chem*., **24**, 767 (2026); https://doi.org/10.1039/D5OB01732G
4. S. Kheirkhahnia, M. Khodi, P. Ahmadfila, S. Ziaei and M. Pordel, *Inorg. Chem. Commun*., **182**, 115460 (2025); https://doi.org/10.1016/j.inoche.2025.115460
5. J. Dong, Q. Zhang, Z. Wang, G. Huang and S. Li, *ChemMedChem*, **13**, 1490 (2018); https://doi.org/10.1002/cmdc.201800253
6. X. Mo, D.P. Rao, K. Kaur, R. Hassan, A.S. Abdel-Samea, S.M. Farhan, S. Bräse and H. Hashem, *Molecules*, **29**, 4770 (2024); https://doi.org/10.3390/molecules29194770
7. R. Nath, S. Ashique, B. Nehra, I. Debnath, S. Ghosh, P.A. Chawla, F. M. Al-Salem, S. Yasmin, M.S. Hussain, A. Chakraborty, A. Chakraborty, L. Das, S.B. Sridhar, J. Das, B. Debnath and M.Y. Ansari, *Mol Divers*., (2026); https://doi.org/10.1007/s11030-026-11499-1
8. A. Catalano, D. Iacopetta, M. S. Sinicropi and C. Franchini, *Appl. Sci*., **11**, 374 (2021); https://doi.org/10.3390/app11010374
9. S. Sadeghian-Rizi, G.A. Khodarahmi, A. Sakhteman, A. Jahanian-Najafabadi, M. Rostami, M. Mirzaei and F. Hassanzadeh, *Res. Pharm. Sci*., **12**, 500 (2017); https://doi.org/10.4103/1735-5362.217430
10. D. Chen, M. Zhao, W. Tan, Y. Li, X. Li, Y. Li and X. Fan, *Eur. J. Pharm. Sci.*, **130**, 100 (2019); https://doi.org/10.1016/j.ejps.2019.01.020
11. C.E. DeSantis, M. Ma, M.M. Gaudet, L.A. Newman, K.D. Miller, A. Goding Sauer, R.L. Siegel and A. Jemal, *CA: Cancer J. Clin.*, **69**, 438 (2019); https://doi.org/10.3322/caac.21583
12. H. Sung, J. Ferlay, R.L. Siegel, M. Laversanne, I. Soerjomataram, A. Jemal and F. Bray, *CA: Cancer J. Clin.*, **71**, 209 (2021); https://doi.org/10.3322/caac.21660
13. C.-R. Zhao, R.-Q. Wang, G. Li, X.-X. Xue, C.-J. Sun, X.-J. Qu and W.-B. Li, *Bioorg. Med. Chem. Lett.*, **23**, 1989 (2013); https://doi.org/10.1016/j.bmcl.2013.02.034
14. X. Zhai, Q. Huang, N. Jiang, D. Wu, H. Zhou and P. Gong, *Molecules*, **18**, 2904 (2013); https://doi.org/10.3390/molecules18032904
15. M. Priyadarshini and N.A.N. Raj, *Photodiagnosis Photodynam. Ther.*, **50**, 104411 (2024); https://doi.org/10.1016/j.pdpdt.2024.104411
16. A. Janem, G. Omar, O. Hamed, S. Jodeh, A. Deghles, A. Berisha, W. Mansour, S.A. Jabal, O. Fares, A. Jaser, A. Amireh and G. Adwan, *Heliyon*, **10**, e33808 (2024); https://doi.org/10.1016/j.heliyon.2024.e33808
17. F.O.A. Frejat, H. Zhai, Y. Cao, L. Wang, Y.A. Mostafa, H.A.M. Gomaa, B.G.M. Youssif and C. Wu, *Bioorg. Chem.*, **126**, 105922 (2022); https://doi.org/10.1016/j.bioorg.2022.105922